energy&fuels

pubs.acs.org/EF Article

Stability, Combustion, and Compatibility of High-Viscosity Heavy Fuel Oil Blends with a Fast Pyrolysis Bio-Oil

Michael D. Kass,* Beth L. Armstrong, Brian C. Kaul, Raynella Maggie Connatser, Samuel Lewis, James R. Keiser, Jiheon Jun, Gavin Warrington, and Dino Sulejmanovic

Cite This: *Energy Fuels* 2020, 34, 8403−8413 Read Online

ACCESS | Metrics & More | Article Recommendations

ABSTRACT: Properties related to the combustion, stability, and compatibility of blends composed of high-viscosity heavy fuel oil (HFO) and highly acidic pyrolysis bio-oil were determined to assess the utility of bio-oil as a marine fuel. The addition of bio-oil was shown to be fully stable with HFO at blend levels up to 50 mass % for up to 2 weeks. Bio-oil concentrations as low as 5 mass % significantly reduced the viscosity of HFO at 25 and 50 °C. Aging studies at 50 and 90 °C showed that the HFO inhibited the polymerization of bio-oil. The heating value and lubricity showed a linear dependency with bio-oil content, and combustion quality was acceptable for blends containing up to 15% bio-oil. The highly acidic bio-oil was found to be corrosive to carbon steel, 2.25Cr-1Mo steel, and 409 stainless steels, but not 304L and 316L. When blended into HFO at levels less than 19 mass %, no measurable corrosion was observed on any of the steel materials, but a 50 mass % concentration produced low-to-moderate corrosion in the carbon steel, 2.25Cr-1Mo steel, and 409 stainless steel grades. The combination of good blend stability, polymerization inhibition, reduced viscosity, and acceptable compatibility for low blend levels suggests that bio-oils may be suitable for use as a marine fuel.

INTRODUCTION

Heavy fuel oils (HFOs) are a class of fuels that are primarily derived from the residuum fraction of refined crude oil. They are also denoted as residual fuel oils and are primarily used as a low-cost fuel for large marine cargo vessels. As a residuum, these fuels are largely composed of high-molecular-weight aromatic and paraffinic hydrocarbons having boiling points in excess of 350 °C. Residual fuel oils are known to contain significant quantities of ash and sulfur and are highly viscous. To better facilitate the handling and processing, they are further blended with lower-viscosity components, which may include lower-viscosity residuals or distillates.[1−4] Even with these additions, residual fuel oils require heating to lower their viscosity to achieve desired flow and combustion characteristics.[1,2] As a result, HFOs are usually defined by their kinematic viscosity at 50 °C, which can range from 180 to 700 cSt.[5,6]

HFOs differ from distillates in that they contain a colloidal dispersion of high-molecular-weight complex polymers (known as asphaltenes) that exist in chemical equilibrium with the surrounding fuel oil.[7−10] The fractions making up HFO are categorized as saturates, aromatics, resins, and asphaltenes (SARA) according to their solubility and adsorption properties.[11,12] Asphaltenes are large polyaromatic carbon ring structures that contain aliphatic side chains. These side structures include carboxylic acids, carbonyls, and phenols and are capable of dipole−dipole and hydrogen bonding.[12] The saturates, aromatics, and resins, which form the surrounding continuous phase, are collectively known as the maltene fraction. The resin fraction is polar, but of lower polarity than the asphaltenes, while the saturates and aromatic fractions are relatively nonpolar. In a complex mixture like residual fuel oil, the asphaltene and surrounding maltene matrix fraction remain as a colloidal dispersion as long as the solubility forces (dispersion, polarity, and hydrogen bonding) between the asphaltene and maltene fractions are similar.[12] Since asphaltenes have high polarity and hydrogen bonding potential, the surrounding maltene fraction must also have similar weak bonding features to maintain a stable suspension. The resins are believed to play a key role in maintaining this equilibrium.[12] The addition of nonpolar solvents (including distillates) to the HFO will lower the solubility of the asphaltenes in solution and can cause them to fall out of solution and precipitate. It is the propensity of asphaltene precipitation from HFO that determines fuel and blend stability. Unstable HFOs are those prone to precipitate asphaltenes, which is the primary cause of filter plugging, fouling, and flow difficulties.

Heavy fuel oil is an important transportation fuel, as it is the predominant fuel for powering marine vessels used to transport goods worldwide. The amount of HFO consumed by the marine sector is estimated at 300 million metric tons per year, which corresponds to approximately 6% of the global demand for oil.[7] However, their high sulfur content means that marine vessels powered by HFO are the largest anthropogenic global

Received: March 10, 2020
Revised: June 1, 2020
Published: June 11, 2020

https://dx.doi.org/10.1021/acs.energyfuels.0c00721
Energy Fuels 2020, 34, 8403−8413

sources of sulfur emissions. HFO is also a significant global contributor to particulate emissions and CO_2. To better reduce worldwide emissions and petroleum consumption, alternative options to HFO are being considered and investigated.

A potential pathway to reduced emissions, improved energy security, and reductions in the carbon intensity is to utilize biofuels in marine shipping. Oxygenated biofuels are inherently low in sulfur and have been shown to reduce particulate emissions.[13] In addition, since they are biomass-derived and renewable in nature, their carbon intensity is low compared to petroleum. A key barrier for many biofuels is the high production cost associated with upgrading. For HFO, this challenge is particularly acute since it is a low-value refinery product and its price is often half that of distillate fuels. However, minimally treated bio-oils, such as fast pyrolysis oils, have potential as a lower-cost biofuel option.[13]

Bio-oils are formed by the fast pyrolysis of biomass, often woody feedstock. The aqueous phase of the raw condensed pyrolysis product is typically removed, leaving behind a more energy-dense, oily water-insoluble fraction (WIF). This WIF is of interest as a potential transportation fuel. The composition is heavily dependent on feedstock and processing conditions, but in general bio-oil contains significant levels of water and organic oxygenates, such as carboxylic acids, phenols, ketones, formaldehydes, and furans and lignin structures.[14−19] As such, bio-oil is inherently highly polar and acidic. The water and oxygenated compounds also reduce the combustion quality of bio-oils, such that they cannot be used to fuel conventional diesel engines.[20,21] As a result, bio-oils require extensive hydrotreating to remove water and acid fractions, thereby improving their combustion quality and enabling them to become soluble with petroleum distillates. This process is energy intensive and expensive, and, as a result, upgraded bio-oil is not economically feasible as an option for distillate fuels. However, because the large 2-stroke crosshead marine engines can operate on poorer combustion quality fuels than conventional diesel engines, bio-oils may have utility as a marine fuel.[22] Also, the high polarity of bio-oil offers the intriguing possibility that it can be blended with HFO without causing the precipitation of asphaltenes.

Information pertaining to the combustion, rheology, and compatibility properties of HFO blended with bio-oil is not widely reported. Two papers were found that evaluated the combustion of pyrolysis oil blends with HFO in burner applications.[23,24] In both studies, a surfactant was added to stabilize the blend, but no information pertaining to the blend characteristics or behavior was reported. A more informative study by Bakhshi and Adjaye indicated that straight blends of pyrolysis oils and HFO were stable for all blend ratios after 24 h of storage. Here, miscibility (or blend stability) was determined by visually observing whether globules had formed in the blends. While these findings are intriguing, they are too limited in scope to adequately assess the viability of HFO/bio-oil blends as marine fuels.

Further studies, characterizing not only blend stability, but also compatibility and combustion behavior, are needed to better understand the opportunities and limitations of blending bio-oil with HFO. In this study, the uniformity and stability of HFO/bio-oil blends were examined along with their viscosity behavior, combustion characteristics, and compatibility with common infrastructure metals. Many of these properties were determined at elevated temperatures to better reflect the operating conditions of existing HFO fuel systems.

DESCRIPTION OF HFO AND BIO-OIL

The HFO used in this study was a high-viscosity, proprietary, research-grade blend developed to have a nominal sulfur content of 0.65 wt %. It was representative of the ISO RMK grade used to fuel cargo vessels.[5,6] Gas chromatography-mass spectrometry (GC-MS) was used to speciate the composition of the HFO. To better ascertain the volatility of the HFO, GC-MS measurements were run for samples heated to 50 and to 90 °C. These results are shown in Figure 1. The resulting GC-MS

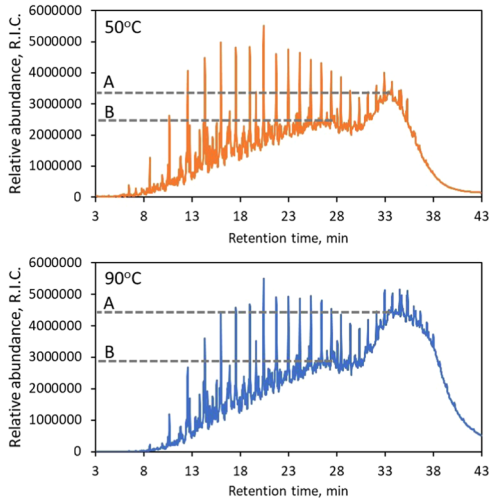

Figure 1. GC-MS profiles for the HFO after being heated to 50 and 90 °C.

results show that the HFO was composed of two distinct fractions: a high-molecular-weight fraction with a peak at point A and a lower-molecular-weight fraction with a peak at point B. The HFO used in this study appears to be composed of two primary blend streams: a heavy residual oil fraction and a lighter (lower-molecular-weight) fraction.

The key properties of the HFO are shown in Table 1 alongside the selected properties of the bio-oil. As can be seen in the table, the two fuel types have very different physical properties. The higher water content and oxygenated components of the bio-oil are primary contributors to the reduced energy content, lower carbon and hydrogen numbers, and higher wear scar diameter of the bio-oil. An interesting feature of bio-oil is that although it has a higher density than the HFO, its viscosity (at 100 °C) is significantly lower than that of HFO. The aqueous modified total acid number (AMTAN) was used to gauge the acidity of the fuels. The AMTAN includes aqueous carrier solvents and is considered more truly representative of the acidity of hydrophilic bio-oils than the total acid number (TAN).[18] The AMTAN results were markedly different for both neat fuels, as shown in Table 1. The low AMTAN for the HFO indicates negligible acidity, which is consistent with residual fuel oil chemistry. In contrast, the AMTAN reading for the bio-oil is quite high and can be considered highly corrosive.

The bio-oil used in this study was sourced from debarked loblolly pine chips and residue.[19] These feedstocks were further processed at the Idaho National Laboratory (INL) Biomass Feedstock National User Facility (BFNUF) and dried to a moisture level below 10 wt %. The bio-oil was synthesized via fast pyrolysis in the Thermochemical Process Development Unit (TCPDU) at the National Renewable Energy Laboratory

https://dx.doi.org/10.1021/acs.energyfuels.0c00721
Energy Fuels 2020, 34, 8403−8413

Table 1. Key Property Measurements for the HFO and Bio-Oil

property	test method	heavy fuel oil	bio-oil
density at 15 °C (g/mL)	ASTM D4052	0.9984 (at 15 °C)	1.22 (at 20 °C)
heat of combustion (gross) (MJ/kg)	ASTM D240	42.90	16.99
aqueous modified total acid number (AMTAN) (mg KOH/g) sample		2	112
heat of combustion (net) (MJ/kg)	ASTM D240	40.72	15.35
flash point (°C)	ASTM D93	94.5	N/A
sulfur content (mass %)	ASTM D2622	0.656	0.009
pour point (°C)	ASTM D5950	6	N/A
viscosity at 50 °C (cSt)	ASTM D445	731.94	N/A
viscosity at 100 °C (cSt)	ASTM D445	41.3	3.133
lubricity (wear scar diameter) (μm)	ASTM D6079	120	440
carbon residue (mass %)	ASTM D44530	16.1	N/A
water content (mass %)	ASTM D6304	0.0287	24.0
sediment (mass %)	ASTM D473	0.02	N/A
ash content (mass %)	ASTM D482	<0.001	<0.05
carbon content (wt %)	ASTM D5291	88.98	44.24
hydrogen content (wt %)	ASTM D5291	10.25	7.71

(NREL). The TCPDU is a half-ton-per-day, pilot-scale plant used to research the thermochemical routes of processing cellulosic biomass to liquid fuels. In this process, the feedstock is crushed to less than 2 mm, entrained in preheated nitrogen gas, and then fed into the 500 °C entrained-flow pyrolysis reactor. Char and ash are removed by cyclones, and the pyrolysis vapors are condensed into oil in the liquid scrubber, which uses dodecane as the scrubbing liquid. After passing through a 10 μm liquid filter, the pyrolysis oil, or bio-oil, is drained off the bottom of a phase separator, while the dodecane recirculates back to the scrubber spray nozzles. The aqueous phase had been removed prior to delivery and the bio-oil appeared to be of uniform consistency.

The chemical specifications of the bio-oil are shown in Table 2 and in Figure 2. As mentioned previously, the acidity for this bio-oil is considered to be high. Formic and acetic acid concentrations were determined via capillary electrophoresis with indirect ultraviolet (UV−visible) absorbance detection, and GC-MS (using a polar column) was used to speciate the hydrocarbon components of the bio-oil. The results in Table 2 show appreciable levels of both formic and acetic acids and other oxygenates (also seen in Figure 2). These oxygenated polar compounds are representative of bio-oils produced from the woody feedstock.

Table 2. Acid Type and Concentration and Key Oxygenates of Bio-Oil

formic acid concentration (mass %)	2.7
acetic acid concentration (mass %)	3.1
methoxymethyl phenol, relative abundance	3.9×10^6
sucrose, relative abundance	2.5×10^7

Bio-oil was added to HFO in mass-percent levels of 5, 10, 15, 20, 25, 50, and 75. In some cases, property measurements (such as heating value) were made at each blend level, while other properties were determined for specific blends. A test matrix listing the properties that were measured and their associated blend contents is shown in Table 3.

The blend samples were prepared by vigorously stirring the bio-oil into the HFO at temperatures around 40 °C for approximately 1 min. Because both the bio-oil and HFO were dark and opaque, it was difficult to determine miscibility by visible observation. This difficulty was also noted in another bio-oil/HFO blend study, where blend stability was assessed by spreading out the blended fuel and looking for evidence of agglomeration. After mixing, the blend samples sat undisturbed for up to several weeks. Subsamples for measurement of sulfur content and heats of combustion were taken by heating the blend samples to 50 °C (to lower the overall viscosity) and pouring out the test volumes. No added mixing step was performed.

To confirm blend uniformity, the sulfur content was determined for each blend level. A linear (or roughly linear) relationship between sulfur content and blend level is indicative of good mixing and blend uniformity. It was not determined whether these blends exist as a single phase (indicating miscibility) or as stable dispersions of one component in the other. The results in Figure 3 show that the sulfur reading for the 75% bio-oil sample deviated significantly from the trend line. This unacceptable deviation indicates that this sample was either not properly mixed or had undergone phase separation. Therefore, the combustion and flow properties that were measured for this sample are not considered to be truly representative of the 75% bio-oil blend with HFO. It is important to note that a second 75% bio-oil blend was prepared for the spot stability test and was considered uniform for test purposes based on uniform flow behavior.

The blend samples that were submitted for sulfur measurement had sat for at least 2 weeks before subsamples were extracted and measurements were taken. While the findings show good blend uniformity, it is possible that the phase separation process was too slow to be manifested in 2 weeks, and that longer storage times are needed to confirm stability.

FUEL BLEND PROPERTIES

Blend Stability. When blending HFO with bio-oil, both asphaltene precipitation and bio-oil polymerization need to be considered. Unlike residual fuel oils, pyrolysis bio-oils are known to polymerize over time, and the rate of formation increases rapidly with temperature.[17,25−28] Associated with polymerization is a marked increase in viscosity, which is a key barrier to the commercialization of bio-oils.[27] The exact mechanisms driving polymerization are unclear, but it is understood that the aldehydes, which have a highly reactive carbonyl end group (as seen in Figure 4), serve as the primary building block for this process. Aldehydes in bio-oil can react with each other (homopolymerize) to form oligomers, but they can also form resins via intermediate reactions with the phenolic and acidic components of bio-oil.[14,17,27]

The standard method for assessing stability or compatibility of residual fuel mixtures is the spot test described in ASTM

https://dx.doi.org/10.1021/acs.energyfuels.0c00721
Energy Fuels 2020, 34, 8403−8413

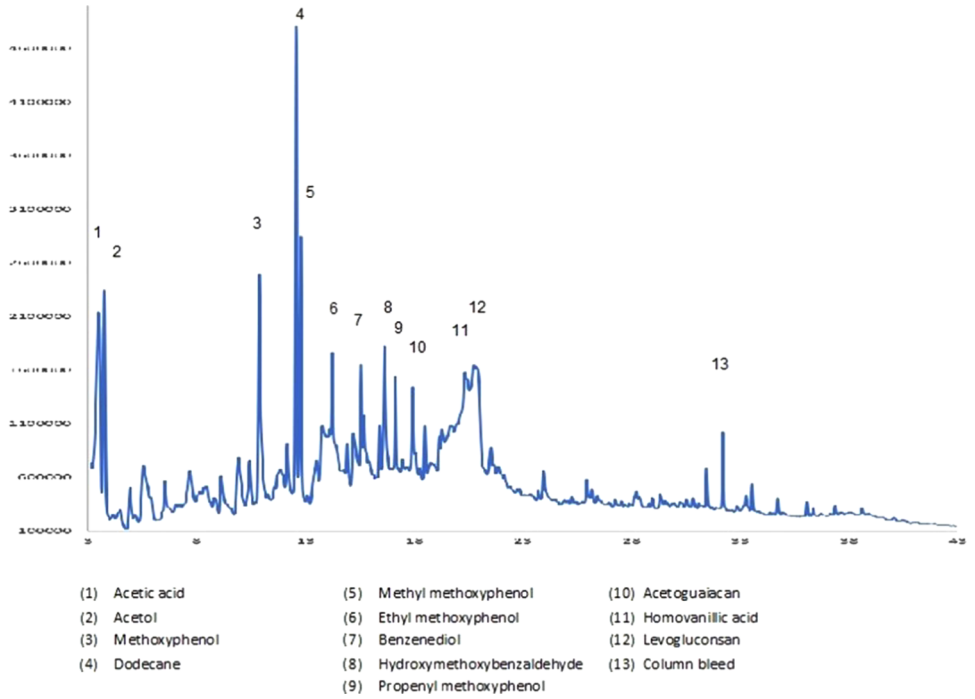

Figure 2. Results of direct thermal sampling, chromatography, and electron ionization mass spectrometry of the bio-oil show significant levels of phenols, residual sugars, and aldehydes.

Table 3. Test Matrix Showing Blend Levels and Their Respective Measured Properties

	blend level of bio-oil in HFO (mass %)								
property	0	5	10	15	20	25	50	75	100
ASTM D4740 spot test	Y					Y	Y	Y	Y
dynamic viscosity	Y	Y	Y	Y		Y			
heating value	Y	Y	Y	Y	Y	Y	Y	Y	Y
combustion analysis	Y	Y	Y	Y					
corrosion/ compatibility	Y		Y[a]		Y[b]	Y	Y		

[a]Actual blend level was 8%. [b]Actual blend level was 19%.

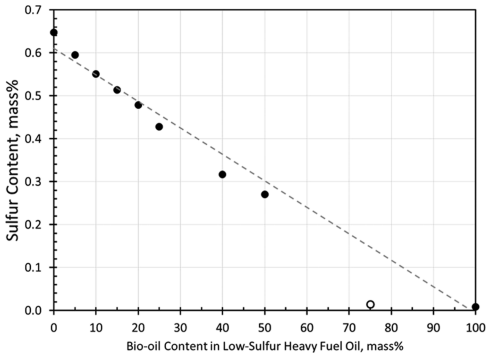

Figure 3. Sulfur content for the HFO blends as a function of bio-oil content.

D4740.[29] In this method, a drop of the sample is placed on a test paper and heated to 100 °C for 1 h. The resulting spots are visually examined for evidence of precipitation (or separation) and graded for compatibility based on the D4740 reference images. The resulting spots for HFO, bio-oil, and HFO blends with 25, 50, and 75% bio-oil are shown in Figure 5. These

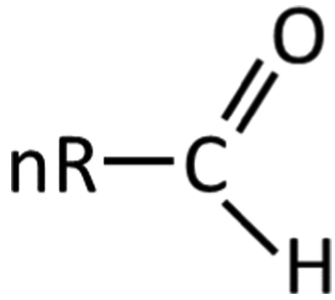

Figure 4. Aldehyde structure showing carbonyl (carbon−oxygen double bond).

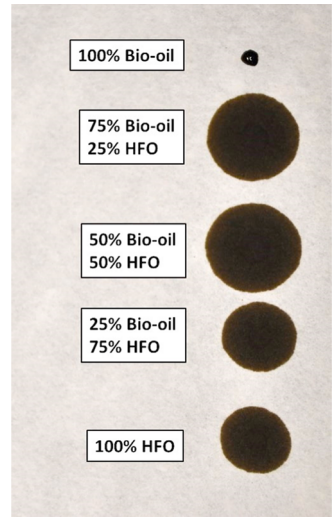

Figure 5. ASTM D4740 spot test results for HFO blended with bio-oil. Blends of HFO containing 0, 25, 50, 75, and 100 mass % bio-oil were evaluated.

https://dx.doi.org/10.1021/acs.energyfuels.0c00721
Energy Fuels 2020, 34, 8403−8413

spots were inspected not only for evidence of asphaltene precipitation, but also for polymerization of the bio-oil fraction. Close inspection of the spots showed that the neat HFO was representative of ASTM D4740 reference images rated as "compatible but requiring careful handling". This rating did not change for blends up to 75% bio-oil. As seen in Figure 5, the neat bio-oil sample was condensed into a hard polymer bead by the heat treatment. Magnification of the bead showed that the surface was smooth and the bead itself was hard (and could not be easily broken). These features are consistent with polymerized bio-oil. No evidence of polymerization was noted for the blended samples. This finding indicates good stability and compatibility of the bio-oil with the HFO. The lack of evidence for asphaltene precipitation indicates that the highly polar bio-oil was able to maintain asphaltene dispersion in the blend.

The mechanisms responsible for the lack of visible polymerization are attributed to dilution and possibly chemical reactions. Diebold and Czernik have shown that adding polar solvents (such as ketones and alcohols) to bio-oils is effective at reducing bio-oil polymerization.[27] This inhibition was attributed to the dilution of the reactive components and solvent reaction with the carbonyl bond of the aldehyde. While the added HFO would have certainly diluted the reactive species of the bio-oil, it is not known if the polar components (resins and asphaltenes) reacted with the aldehydes to inhibit oligomer formation.

In addition to the spot test, other, less-subjective, properties relating to compatibility and handling were evaluated. These include determination of viscosity and lubricity measurements.

Dynamic Viscosity Results and Influence of Bio-Oil Content and Elevated Temperature. Viscosity measurements were performed to assess the flow dynamics of HFO blended with bio-oil. A significant viscosity increase accompanying bio-oil additions would potentially damage pumps and overpressure fuel lines. To assess flow performance, the dynamic viscosities for the HFO and its blends with bio-oil were measured at 25, 50, and 90 °C. Rheological data were acquired using a thermal analysis (TA) Instruments AR-G2 controlled stress rheometer (New Castle, DE). The temperature was controlled using a steel Peltier plate, while a 40 mm cone and plate assembly were used to measure viscosity and stress as a function of the shear rate. A flow sweep from 3 to 37 Pa was performed for each temperature setting. To study aging effects, the second set of experiments was performed in which the HFO blends were stored in porcelain crucibles and placed inside a Thermolyne 1400 box furnace (Waltham, MA) at 50 or 90 °C and aged up to 5 days at the selected temperature. A flow sweep at the desired temperature was completed daily during the aging period.

The test temperatures of 50 and 90 °C correspond to the operating temperatures of the vessel fuel storage and settling tanks and the purifier. These curves are plotted in Figures 6−8. HFO exhibits generally Newtonian flow behavior at low-to-moderate shear rates (0.1 to 100/s) and shear thinning at rates greater than 100/s. However, as seen in Figure 6, the viscosity behavior of HFO was dramatically affected by the added bio-oil. The addition of 5% bio-oil was found to lower the viscosity from 15 to 16 Pa·s to values approaching 6 Pa·s, which is less than half the value of neat HFO. Increasing the bio-oil blend level to 10% produced a similar result, although the viscosity at low shear rates was higher than for the blend containing 5% bio-oil. The addition of 15 and 25% bio-oil produced similar

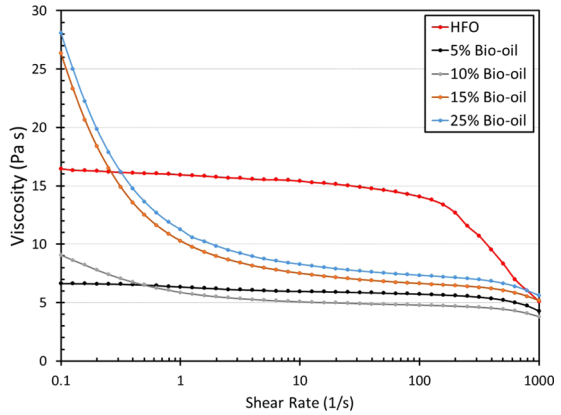

Figure 6. Dynamic viscosity results at 25 °C for HFO blended with bio-oil.

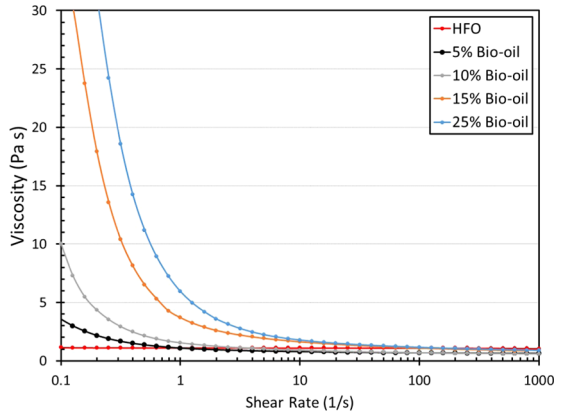

Figure 7. Dynamic viscosity results at 50 °C for HFO blended with bio-oil.

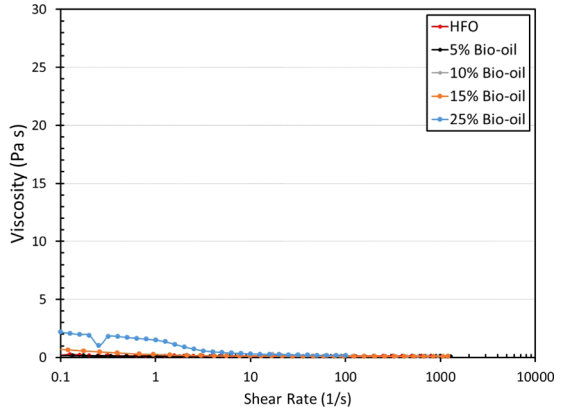

Figure 8. Dynamic viscosity results at 90 °C for HFO blended with bio-oil.

curves, and both produced noticeably higher viscosities than HFO at very low shear rates. As the shear rate increased, the viscosity values for these blends dropped rapidly and, for rates greater than 1/s, the viscosities had dropped well below that of the HFO.

The rheological behavior of several neat (unblended) bio-oils has been reported as Newtonian over a large shear span.[15] The influence of the HFO on the non-Newtonian flow behavior of the HFO bio-oil blends at low shear rates is evident and consistent with other reported bio-oil blended

https://dx.doi.org/10.1021/acs.energyfuels.0c00721
Energy Fuels 2020, 34, 8403−8413

slurries.[30,31] The viscosity measurements at 50 °C (Figure 7) show that for shear rates greater than 10/s, the viscosity behavior for HFO and its blends with bio-oil are similarly Newtonian and converge to a viscosity value around 1 Pa·s. At 50 °C, the viscosity was observed to increase with bio-oil content at very low shear rates. At higher shear rates, the blend viscosities converge to the measured HFO values and exhibit shear thinning behavior. The implication is that low-speed pumping systems may require some modification to handle the increased viscosity of the blends. However, medium-to-higher-speed pumps would likely be acceptable for operation at 50 °C. For the 90 °C condition (Figure 8), HFO containing up to 15% bio-oil produced negligible viscosity values. However, the blend containing 25% bio-oil did produce a small viscosity increase for shear rates less than 10/s.

Aging as a Function of Temperature and Bio-Oil Content. The viscosities of HFO and bio-oil/HFO blends were measured as a function of time to determine if aging at temperature affected the flow behavior. HFO and bio-oil blends at loadings of 5, 10, 15, and 25% bio-oil were heated to 50 and 90 °C, and the samples were periodically removed for rheological characterization. A flow sweep of viscosity as a function of the shear rate was conducted at varying time intervals from 4 h up to 96 h. For the samples held at 50 °C, the viscosity behavior was obtained for shear rates between 2 and 40/s, while the samples at 90 °C required higher shear rates (20−400/s) to elucidate behavior. Because of the different ranges in frequency sweeps, temperature comparisons were conducted at 10/s and 100/s for the 50 and 90 °C temperature settings, respectively. In general, all samples at either temperature condition showed Newtonian flow behavior except at higher shear rates where the viscosity increased slightly.

The viscosity versus the run time is shown in Figure 9 for each test temperature and biofuel content. As can be seen in the figure, the measured viscosities were higher for test fuels maintained at 50 °C than those held at 90 °C. In both cases, the viscosity measurements are low. HFO and its blends with bio-oil exhibited a slight increase in viscosity with exposure time for each temperature setting. At 50 °C, a small marginal increase in viscosity was noted when bio-oil was added at levels of 5, 10, and 15%. For these blend levels, the measured viscosities were essentially the same, while the addition of 25% bio-oil caused a slight additional increase. At 90 °C, the viscosity increase accompanying the bio-oil additions was much more pronounced. Here, the 5 and 25% bio-oil blends produced similar results, while the measured viscosities for the 10 and 15% blends were very similar. In both instances, there was no definitive trend of increasing viscosity with bio-oil content. The results also show that when bio-oil was added to HFO in levels up to 25%, no additional increase in viscosity was observed after 72 h of exposure time. This lack of viscosity increase (compared to neat HFO) is another strong indication that polymerization of the bio-oil was inhibited.

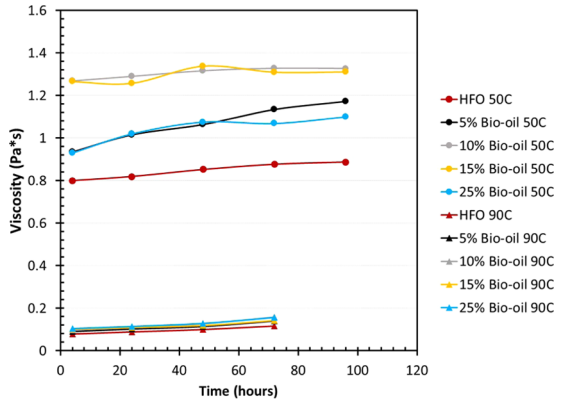

Figure 9. Dynamic viscosity results for HFO blends at exposure temperatures of 50 and 90 °C. Bio-oil contents are expressed in mass %.

The viscosities of heavy fuel oils are typically reduced by adding distillate cutter stock. Distillates have much lower viscosities than residual fuel oils and they reduce the overall viscosity through dilution. Because the bio-oil used in this study had much lower viscosity than the HFO, the dilution effect explains the reduced viscosity of the fuel blends. It is important to note that dramatic reductions in viscosity can be achieved via dilution, even for small additions. For instance, Badger and Schobert reported four-fold viscosity reductions in heavy crude oils by adding only 5% of either toluene, xylene, or cumene.[32]

Lubricity Behavior. The lubricity of the test fuels was assessed via wear scar diameter measurements, as shown in Figure 10. The wear scar diameter (WSD) is inversely proportional to lubricity. As seen in the figure, HFO produces a much smaller WSD than neat bio-oil, indicating better lubricity. The data in Figure 10 show a roughly linear relationship between WSD and bio-oil blend levels. Lubricity is an important property used in the material selection and design of fuel pumps, valves, meters, and piping systems. A reduction in lubricity may lead to an increase in the wear rate of metallic components in these systems.

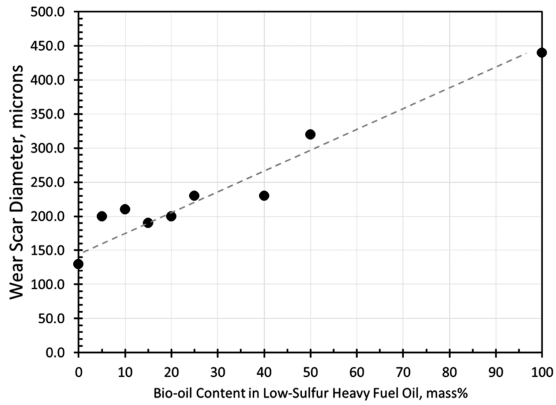

Figure 10. Wear scar diameter results for HFO blends with bio-oil.

HEATING VALUE AND COMBUSTION BEHAVIOR

Heating Value of HFO Bio-Oil Blends. The gross and net heating values of the HFO/bio-oil blends are shown in Figure 11 and exhibit a strong linear relationship with bio-oil content. This linear relationship, along with that of the sulfur content (as seen in Figure 3), lends credence that the bio-oil in these samples was uniformly dispersed in the HFO.

The combustion quality was further assessed by testing the blend samples in an FIA-100 FCA fuel combustion analyzer to determine the estimated cetane number (ECN).[22] For heavy fuel oils (or residual fuels), the ECN is the primary parameter used to assess the combustion quality. For two-stroke

https://dx.doi.org/10.1021/acs.energyfuels.0c00721
Energy Fuels 2020, 34, 8403−8413

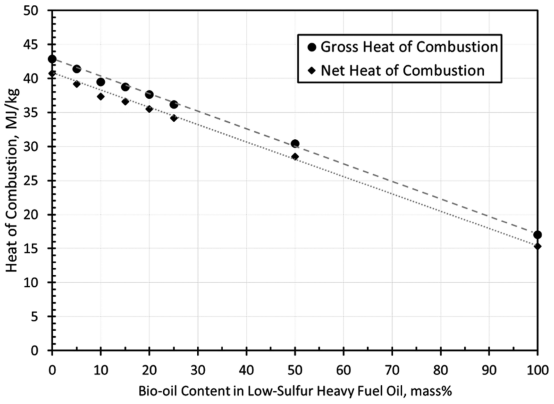

Figure 11. Relationship between heat of combustion and bio-oil concentration in the HFO.

crosshead marine engines, ECN values greater than 10 are considered acceptable for normal operation. Four-stroke engines are more sensitive to fuel quality, and ECNs of less than about 14 may produce operational difficulties.[22] The fuel combustion analyzer also provides information related to the ignition, combustion, and post-combustion characteristics of the HFO being tested. The method measures the pressure rise during ignition and combustion in a constant volume chamber. From this information, the rate of heat release is determined using the first law of thermodynamics, and the ECN is calculated from the main combustion delay (MCD), according to eq 1

$$\mathrm{ECN} = 153.15e^{-0.2861\mathrm{MCD}} \quad (1)$$

MCD is the time interval (in ms) required for the pressure to reach 10% of the maximum pressure. High ECN values correspond to short main combustion delays and therefore more favorable combustion behavior.

Combustion Characteristics. The injector of the test apparatus failed to properly inject the fuel for blend levels containing higher than 15% bio-oil. The results for HFO and its blends with 5, 10, and 15 mass % bio-oil are listed in Table 4.

The pressure and rate of heat release (ROHR) profiles for these blends are shown together in Figure 12. The curves for HFO and its blends with 5 and 10% bio-oil exhibit similar pressure and ROHR profiles. For these blends, a distinct rise in the ROHR precedes the main (bulk) heat release during combustion. This feature is normally indicative of two-stage ignition and further confirms that the HFO contains two fractions that have distinct ignition characteristics, which are likely due to two different boiling ranges. This feature is not uncommon in many HFO fuels,[22] especially when a heavy residuum fraction is blended with a lower-boiling-point distillate. These combustion characteristics are considered appropriate for use in marine engines, but a more continuous combustion profile is preferred. When the blend level of the bio-oil is increased to 15%, the combustion profile changes such that the peak pressure and ROHR are significantly reduced. The other notable feature is that the early ignition event becomes less pronounced than for the lower-level blends.

The ignition and main combustion delay for the blends are shown in Figure 13. The ignition delay is relatively constant (unaffected) for the different blends, indicating that the presence of bio-oils at these levels did not influence (or quench) the start of combustion. The main combustion delay

Table 4. Fuel Ignition and Combustion Parameters for HFO and its Blends With Bio-Oil

combustion parameter	100% HFO	95% HFO, 5% bio-oil	90% HFO, 10% bio-oil	85% HFO, 15% bio-oil
estimated cetane number	23.3	21.6	21.1	17.9
ignition delay (ms)	5.36	5.49	5.36	5.48
main combustion delay (ms)	6.58	6.84	6.93	7.50
end of main combustion (ms)	10.77	11.03	11.52	13.43
end of combustion (ms)	15.17	16.12	17.62	21.14
precombustion period (ms)	1.23	1.35	156	2.02
main combustion period (ms)	4.19	4.18	4.59	5.93
after-burning period (ms)	4.39	5.09	6.09	7.71
maximum ROHR (bar/ms)	3.31	3.24	3.03	2.17
position of max ROHR (ms)	7.28	7.60	7.69	8.43
accumulated ROHR (bar)	7.31	7.21	7.39	6.75
maximum pressure rise (bar)	7.46	7.35	7.54	6.89

(which denotes the start of the main combustion event) was influenced by the bio-oil additions. The addition of 5 and 10% bio-oil increased the delay time by 0.26 and 0.35 ms, respectively. However, the addition of 15% bio-oil caused a more pronounced increase (0.92 ms) in combustion delay. Although the point of initial ignition is not affected by the bio-oil additions, the main combustion process or bulk combustion event is delayed (slowed down) by the bio-oil. This is not surprising since the bio-oil lowers the blend heating value and contains water and oxygenates that impede bulk combustion.[21] The initial ignition is a more localized event and therefore is not as impacted by the added bio-oil. As seen in Figure 13, the precombustion period was only slightly increased by the added bio-oil. This provides further evidence that the early ignition characteristics are more localized in nature, as can also be seen by the ignition delay behavior.

The ECN for the neat HFO was measured to be 23.3. This value was lowered to 21.6 and 21.1 with additions of 5 and 10% bio-oil, respectively. A further reduction to 17.9 was noted when the bio-oil level was increased to 15%. These ECN values are considered acceptable for use in two-stroke engines by CIMAC.[22] However, for four-stroke engines, only 5 and 10% additions are fully acceptable. For blends containing 15% bio-oil, difficulties may be encountered using four-stroke engines under low-load operating conditions.

Additional parameters associated with the combustion event are shown in Figure 14. Interestingly, the main combustion period was relatively unaffected by bio-oil additions of 5 and 10%, but 15% produced a pronounced increase in the combustion period. This increase indicates that bio-oil levels of 15% will effectively slow down the overall combustion process. The end of main combustion, the end of combustion, and the after-burning period are observed to increase slightly with bio-oil content up to 10%. The addition of 15% bio-oil produced a more pronounced increase in these combustion parameters.

https://dx.doi.org/10.1021/acs.energyfuels.0c00721
Energy Fuels 2020, 34, 8403−8413

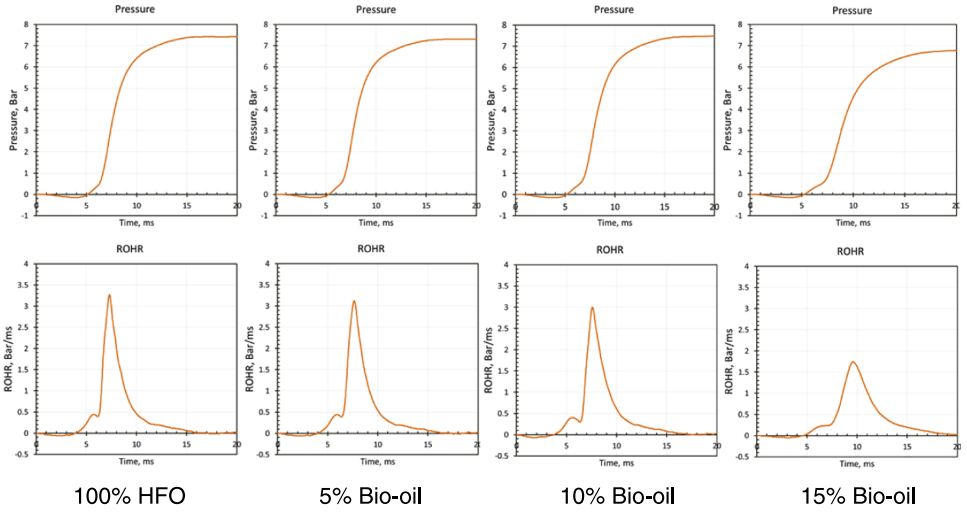

Figure 12. Combustion pressure and ROHR profiles of HFO and its blends with bio-oil obtained from the IP541/06 test method for determining ECN from heavy residual fuels.

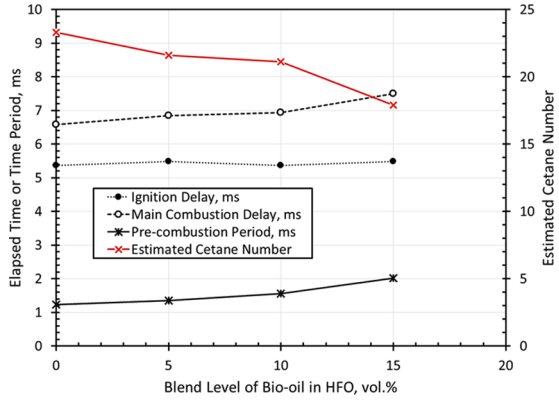

Figure 13. Ignition and combustion delay, precombustion period, and estimated cetane number of HFO and its blends with 5, 10, and 15% bio-oil.

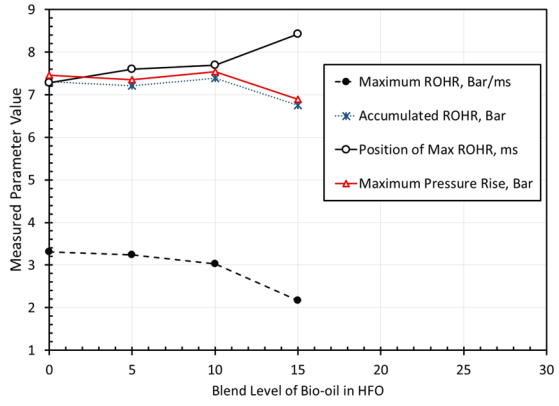

Figure 15. Parameters associated with the rate of heat release and maximum cylinder pressure for HFO and its blends with 5, 10, and 15% bio-oil.

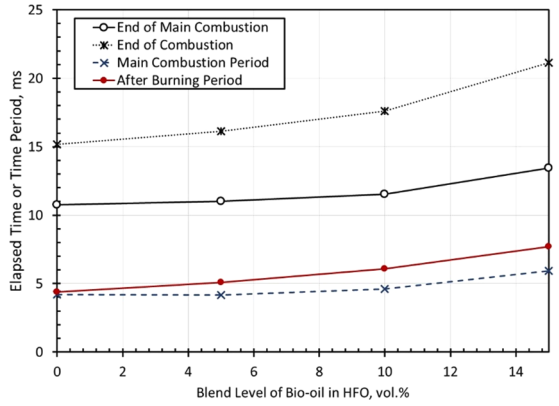

Figure 14. Times associated with the end of main and total combustion and the elapsed time associated with main combustion and after-burning periods for HFO and its blends with 5, 10, and 15% bio-oil.

The peak pressures measured for HFO and its bio-oil blends are shown in Figure 15 along with the key ROHR parameters. These results show that the trends in peak pressure and accumulated ROHR are similar. In both cases, the pressure and accumulated ROHR are relatively unaffected by bio-oil additions of 5 and 10%. However, a noticeable decrease occurred when the bio-oil content was increased to 15%. In contrast, the maximum ROHR and its position showed more sensitivity to the lower blend levels (5 and 10%). Here, the maximum ROHR showed a small decrease up to 10% bio-oil while the corresponding time to reach maximum value was lengthened. As with the other combustion parameters, a more pronounced effect on maximum ROHR was observed with 15% bio-oil. The profiles of these combustion parameters align with those shown in Figures 13 and 14 and indicate that combustion kinetics for HFO having blend levels less than 10% bio-oil are significantly altered when the bio-oil level reaches 15%.

COMPATIBILITY WITH CARBON AND STAINLESS STEELS

Because bio-oils contain appreciable levels of water and carboxylic acids, they are known to be corrosive to mild steels.[33] To evaluate the corrosivity of HFO blends with bio-oil, a series of experiments were conducted, which evaluated different steel types and specimen types with HFO-containing bio-oil in mass fractions of 8, 19, 25, and 50% as well as a neat bio-oil. The AMTAN results for the HFO and the bio-oil blends are shown in Figure 16. The AMTAN numbers for the

https://dx.doi.org/10.1021/acs.energyfuels.0c00721
Energy Fuels 2020, 34, 8403−8413

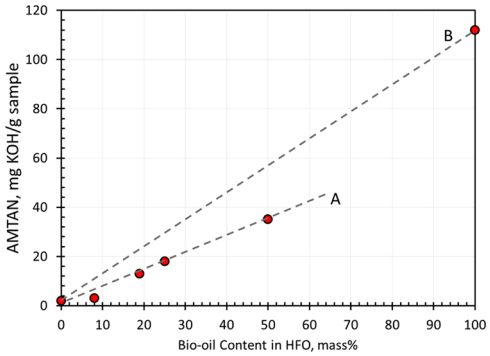

Figure 16. AMTAN results for blends of bio-oil with HFO.

fuel blends indicated low acidity and tended to have a linear relationship with the bio-oil content, as seen by the trend line A. These values are less than would be achieved if a straight-line relationship existed with concentration, as indicated by trend line B.

The materials that were evaluated were five common structural steels (carbon steel, 2.25Cr-1Mo steel, 409 stainless steel, 304L stainless steel, and 316L stainless steel). The composition of these steels is shown in Table 5. As can be seen

Table 5. Type and Nominal Elemental Composition of the Steel Materials as Listed in the Metals Handbook[34]

alloy	Fe (wt %)	Cr (wt %)	Ni (wt %)	Mo (wt %)	Mn (wt %)	C (wt %)
carbon steel	balance				1.0	0.13
2.25Cr-1Mo	balance	2.25		1.0	0.4	0.1
409 stainless steel	balance	11			0.3	0.015
304L stainless steel	balance	18.3	9.0		1.7	0.02
316L stainless steel	balance	16.4	10.2	2.1	1.6	0.02

in the table, the chromium concentration is variable among the steel grades. Chromium is added to steel to improve its overall corrosion resistance to acids, and the stainless steel (SS) grades having the Cr content above 11 wt % (to form a Cr_2O_3-rich passive surface layer) would be expected to have the best resistance to corrosion.

The test samples included unstressed sheet coupons and U-bend stressed specimens, as shown in Figure 17. The materials were supplied by Metal Samples Company (Alabama Specialty Products, Inc.) of Munford, Alabama. The thickness, width, and length of the sheet (bar) coupons measured 1.59 mm (0.0625 in.), 15.9 mm (0.625 in.), and 31.75 mm (1.25 in.), respectively, with a 6.35 mm (0.25 in.) diameter mounting hole, as shown. The U-bend specimens were 1.59 mm (0.0625 in.) thick × 1.27 mm (0.50 in.) wide × 85.725 mm (3.375 in.) long with two 6.35 mm (0.25 in.) diameter mounting holes.

The specimens were exposed in HFO, bio-oil, and their blends for 500 h at 50 °C. The exposure chambers were equipped with a condenser in the vapor region to collect and return volatile organic components to the liquid phase. Argon was used as the cover gas. One set of specimens was immersed in the liquid phase of the test fuels, while a second set was placed in the vapor phase (that existed above the surface level of test fuels).

The corrosion results for the five steel materials are shown in Tables 6 and 7 for the specimens that were immersed in the

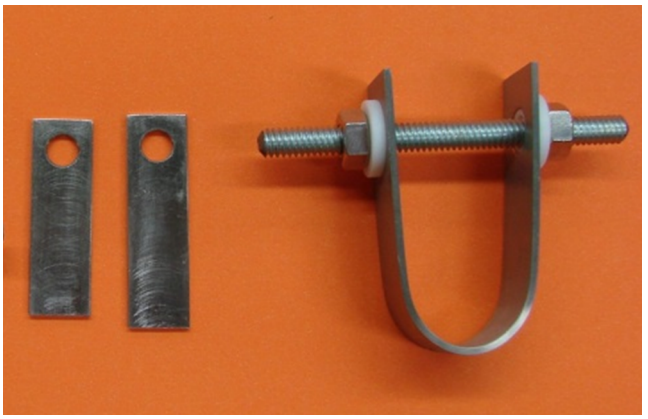

Figure 17. Photograph showing specimen geometries; unstressed alloy coupons (left two) and the U-bend sample (right). The distance of each end in the U-bend sample was approximately 2.5 cm (1 in.).

Table 6. Measured Corrosion Rates for Steels Exposed in the Liquid Fuel Blends for 500 h

bio-oil content (mass %)	carbon steel	2.25Cr-1Mo steel	409 stainless steel	304L stainless steel	316L stainless steel
8	<0.01	<0.01	<0.01	<0.01	<0.01
19	<0.01	<0.01	<0.01	<0.01	<0.01
25	0.03	0.07	<0.01	<0.01	<0.01
50	0.04	0.05	0.04	<0.01	<0.01
100	1.69	2.83	0.94	<0.01	<0.01

Table 7. Measured Corrosion Rates for Steels Exposed in the Vapor Phase of the HFO Bio-oil Blends for 500 h

bio-oil content (mass %)	carbon steel	2.25Cr-1Mo steel	409 stainless steel	304L stainless steel	316L stainless steel
8	0.04	<0.01	<0.01	<0.01	<0.01
19	0.04	<0.01	<0.01	<0.01	<0.01
25	0.03	0.04	<0.01	<0.01	<0.01
50	0.02	<0.01	<0.01	<0.01	<0.01
100	0.44	0.44	0.04	<0.01	<0.01

test fuel liquid and vapor spaces, respectively. The corrosion rate of the carbon steel, 2.25Cr-1Mo steel, and 409 SS specimens with the neat bio-oil (100%) was considered high (>0.25 mm/yr) and was typical of bio-oil exposures with these steel grades.[31] Negligible corrosion (<0.01 mm/yr) was noted for 304L and 316L stainless steels. The highest corrosion rates occurred for the carbon steel and the 2.25%Cr-1Mo steel grades. For these two steel types, moderate corrosion (between 0.01 and 0.25 mm/yr) was observed for HFO blended with 25 and 50% bio-oil, but high corrosion rates were measured for the specimens exposed to 100% bio-oil. The 409 stainless steel specimens underwent moderate corrosion when exposed to the 50% bio-oil blend, while those exposed to neat bio-oil exhibited high corrosion rates (>0.25 mm/yr). Onboard HFO fueling systems are primarily composed of carbon steels and stainless steels. These results show that tanks and piping composed of carbon steel, 2.25Cr-1Mo steel, and 409 stainless steel are prone to corrosion in the neat bio-oil, but that 304L and 316L are suitable for use.

Interestingly, the carbon steel specimens exposed to the vapor phase experienced measurable corrosion for test fuels containing lower (8 and 19 mass %) bio-oil contents,

https://dx.doi.org/10.1021/acs.energyfuels.0c00721
Energy Fuels 2020, 34, 8403−8413

compared to negligible corrosion in the liquid phase. In contrast, the carbon steel specimens exposed to neat bio-oil showed much higher corrosion for the liquid versus the vapor phase exposures. The most likely reason for the increased corrosivity in the vapor phase is due to the higher vapor pressures of the acid and water components of the bio-oil. The higher volatility of the acetic acid and water means that the vapor region will have higher levels of these corrosive species relative to the liquid fuel blend. For the neat bio-oil, there is no HFO to dilute the bio-oil's acidic components in the liquid phase. Therefore, the corrosion rate is higher in the liquid phase. Analysis of the U-bend specimens showed no evidence of stress-accelerated corrosion on any of the alloy specimens exposed to the test fuels, including the 100% bio-oil exposure.

■ CONCLUSIONS

In this study, a high-viscosity, low-sulfur heavy fuel oil was successfully blended with highly acidic bio-oil derived via fast pyrolysis of pine feedstock. The ASTM D4740 spot test results showed blend uniformity between the two fuel types and that asphaltene precipitation was not promoted by the added bio-oil. When blended at levels as low as 5 mass %, the bio-oil was able to dramatically lower the viscosity of the HFO at 25 and 50 °C. This feature further confirms bio-oil compatibility with HFO. Perhaps, more importantly, significant energy and cost savings can be realized by reducing the level of heating needed to reduce the viscosity of HFO with the addition of bio-oil. An aging study showed that the blend viscosities were unaffected by continuous operation at extended periods. This finding (along with the other stability tests) shows that the polymerization of bio-oil was inhibited by the HFO. The measured lubricity values of bio-oil were lower than for HFO and showed a linear relationship with the blend level. The heating value, or energy content, of the blends also showed a linear behavior with bio-oil content. These linear relationships with bio-oil content further infer uniformity of the fuel blends.

The combustion quality was successfully assessed for HFO-containing low blend levels. Bio-oil lowered the estimated cetane number, but acceptable combustion quality was achieved for blends up to 15% bio-oil. The pressure and ROHR profiles were very similar for HFO and bio-oil blends of 5 and 10%. The addition of 15% bio-oil produced a pronounced drop in peak pressure and peak ROHR.

Corrosion tests conducted on selected structural alloys showed that unacceptable corrosion may occur for carbon steel, 2.25Cr-1Mo steel, and 409 stainless steels when exposed to neat bio-oil. The corrosion rates for 304L and 316L steels with the neat bio-oil were negligible. For HFO blended with bio-oil at levels below 19%, no measurable corrosion was reported for any of the steel materials. However, when the bio-oil content was increased to 50%, low-to-moderate corrosion rates were obtained for carbon steel, 2.25Cr-1Mo steel, and the 409 stainless steel grades. The carbon steel also showed measurable corrosion with a blend containing 25% bio-oil. The corrosion rates were observed to increase for carbon steels exposed to the vapor phase of the 8 and 19% bio-oil blends with HFO, indicating that the acidity was higher in this region.

■ AUTHOR INFORMATION

Corresponding Author

Michael D. Kass − *Fuels, Engines and Emissions Research Center, Oak Ridge National Laboratory, Oak Ridge, Tennessee 37830, United States;* orcid.org/0000-0001-9072-2100; Phone: 865-341-1241; Email: kassmd@ornl.gov

Authors

Beth L. Armstrong − *Fuels, Engines and Emissions Research Center, Oak Ridge National Laboratory, Oak Ridge, Tennessee 37830, United States;* orcid.org/0000-0001-7149-3576

Brian C. Kaul − *Fuels, Engines and Emissions Research Center, Oak Ridge National Laboratory, Oak Ridge, Tennessee 37830, United States*

Raynella Maggie Connatser − *Development Division, Y-12 National Security Complex, Oak Ridge, Tennessee 37830, United States*

Samuel Lewis − *Fuels, Engines and Emissions Research Center, Oak Ridge National Laboratory, Oak Ridge, Tennessee 37830, United States*

James R. Keiser − *Fuels, Engines and Emissions Research Center, Oak Ridge National Laboratory, Oak Ridge, Tennessee 37830, United States*

Jiheon Jun − *Fuels, Engines and Emissions Research Center, Oak Ridge National Laboratory, Oak Ridge, Tennessee 37830, United States;* orcid.org/0000-0001-9500-5637

Gavin Warrington − *Fuels, Engines and Emissions Research Center, Oak Ridge National Laboratory, Oak Ridge, Tennessee 37830, United States*

Dino Sulejmanovic − *Fuels, Engines and Emissions Research Center, Oak Ridge National Laboratory, Oak Ridge, Tennessee 37830, United States*

Complete contact information is available at: https://pubs.acs.org/10.1021/acs.energyfuels.0c00721

Author Contributions

The manuscript was written through the contributions of all authors. All authors have given approval to the final version of the manuscript. These authors contributed equally.

Funding

This material is based upon work supported by the U.S. Department of Energy's Office of Energy Efficiency and Renewable Energy (EERE) Bioenergy Technologies Office (BETO) under the Award Number DE- AC05-00OR22725.

Notes

The authors declare no competing financial interest.

■ ACKNOWLEDGMENTS

The authors gratefully acknowledge the efforts of Alexander Rogers and Andres Marquez-Rossy of the Oak Ridge National Laboratory for their assistance in the operation of the stress rheometer and subsequent data collection. Special acknowledgments are also extended to Daniel Carpenter and Kristin Smith of the National Renewable Energy Laboratory for providing the bio-oil used in this study. We would also like to

https://dx.doi.org/10.1021/acs.energyfuels.0c00721
Energy Fuels 2020, 34, 8403−8413

acknowledge the helpful contributions of three anonymous reviewers, which greatly improved the quality of the final manuscript. This material is based upon work supported by the U.S. Department of Energy's Office of Energy Efficiency and Renewable Energy (EERE) Bioenergy Technologies Office (BETO) under the Award Number DE- AC05-00OR22725.

REFERENCES

(1) CONCAWE. *Heavy Fuel Oils*, Report No. Product Dossier No. 98/109. Brussels, 1998.
(2) *Notes of Heavy Fuel Oil by the American Bureau of Shipping, ABS Plaza, 16855 Northchase Drive, Houston, TX 77060 USA*; 2001.
(3) American Bureau of Shipping. *Notes on Heavy Fuel Oil. Houston, TX*; 1984.
(4) Thomas, J. F.; Sluder, C. S.; Kass, M. D.; Theiss, T. T. *A Guide to Fuel, Lubricant, and Engine Concerns Relative to the IMO 2020 Fuel Oil Sulfur Reduction Mandate*, Oak Ridge National Laboratory Report No. ORNL/SPR-2019/1406; 2019.
(5) ISO 8217. *Petroleum Products—Fuels (class F)—Specifications of Marine Fuels*; 2017.
(6) ISO 8216-1. *Petroleum Products—Fuels (class F)—Classification—Part 1: Categories of Marine Fuels*; 2017.
(7) CONCAWE. Marine Fuel Facts 2017. https://www.concawe.eu/wpcontent/uploads/2017/01/marine_factsheet_web.pdf (accessed Jan 4, 2020).
(8) Jun, W. H.; John, O. O.; You, L. P.; Guang, J. F. Understanding Asphaltenes Stability in Marine Fuel Oil Through Separability Number. *Information Technology Journal* **2013**, *12*, 8510−8513.
(9) Hofko, B.; Eberhardsteiner, L.; Fu, J.; Grothe, H.; Handle, F.; Hospodka, M.; Grossegger, D.; Nahar, S.; Schmets, A.; Scarpas, A. Impact of maltene and asphaltene fraction on mechanical behavior and microstructure of bitumen. *Materials and Structures* **2016**, *49*, 829−841.
(10) Rogel, E.; Leon, O.; Espidel, Y.; Gonzalez, Y. Asphaltene Stability in Crude Oils. *Society of Petroleum Engineers* **2001**, *16*.
(11) Garaniya, V.; McWilliam, D.; Goldsworthy, L.Chemical Characterization of Heavy Fuel Oil for Combustion Modeling. *Proceedings of the World Engineers***2011**.
(12) McKay, J.; Amend, P.; Cogswell, T.; Harnsberger, P.; Erickson, R.; Latham, D. In Petroleum Asphaltenes: Chemistry and Composition, Energy Research and Development Administration, Analytical Chemistry of Liquid Fuel Sources. *Advances in Chemistry*; American Chemical Society: Washington, DC, 1978.
(13) Kass, M.; Abdulla, Z.; Biddy, M.; Drennan, C.; Hawkins, T.; Jones, S. et al. *Understanding the Opportunities of Biofuels for Marine Shipping*, Oak Ridge National Laboratory Report No. ORNL/TM-2018/1080; 2018.
(14) Lu, Q.; Li, W.; Zhu, X. Overview of Fuel Properties of Biomass Fast Pyrolysis Oils. *Energy Conversion and Management* **2009**, *50*, 1376−1383.
(15) Nolte, M.; Liberatore, M. Viscosity of Biomass Pyrolysis Oils from Various Feedstocks. *Energy Fuels* **2010**, *24*, 6601−6608.
(16) Czernik, S.; Bridgwater, A. Overview of Applications of Biomass Fast Pyrolysis Oil. *Energy Fuels* **2004**, *18*, 590−598.
(17) Diebold, J. *A Review of the Chemical and Physical Mechanisms of the Storage Stability of Fast Pyrolysis Bio-Oils*, National Renewable Energy Laboratory Report No. NREL/SR-570-27613; 2000.
(18) Connatser, R.; Lewis, S.; Keiser, J.; Choi, J. Measuring Boi-oil Upgrade Intermediates and Corrosive Species with Polarity-Matched Analytical Approaches. *Biomass and Bioenergy* **2014**, *70*, 557−563.
(19) Klinger, J.; Carpenter, D.; Thompson, V.; Yancey, N.; Emerson, R.; Gaston, K.; et al. Pilot Plant Reliability Metrics for Grinding and Fast Pyrolysis of Woody Residues. *ACS Sustainable Chemistry & Engineering* **2020**, *8*, 2793−2805.
(20) Mueller, C. The Feasibility of Using Raw Liquids from Fast Pyrolysis of Woody Biomass as Fuels for Compression-Ignition Engines: A Literature Review. *SAE Int. J. Fuels Lubr.* **2013**, *6*, 251−262.
(21) Shihadeh, A.; Hochgreb, S. Diesel Engine Combustion of Biomass Pyrolysis Oils,". *Energy Fuels* **2000**, *14*, 260−274.
(22) *CIMAC Fuel Quality Guide—Ignition and Combustion*, International Council on Combustion Engines; 2011.
(23) Hou, S.; Huang, W.; Rizal, F.; Lin, T. Co-firing of Fast Pyrolysis Bio-oil and Heavy Fuel Oil in a 300-kW Furnace. *Appl. Sci.* **2016**, *6*, 1−11.
(24) Kuan, Y.; Wu, F.; Chen, G.; Lin, H.; Lin, T. Study of the Combustion Characteristics of Sewage Sludge Pyrolysis Oil, Heavy Fuel Oil, and Their Blends. *Energy* **2020**, *201*, No. 117559.
(25) Bakhshi, N.; Adjaye, J. In *Properties and Characteristics of Ensyn Bio-oil*, Proceedings of the Biomass Pyrolysis Oil Properties Combustion Meeting, Milne, T. NREL Report No. NREL-CP-430-7215, pp 54−66.
(26) Hu, X.; Wang, Y.; Mourant, D.; Gunawan, R.; Lievens, C.; Chaiwat, W.; Gholizadeh, M.; Wu, L.; Li, X.; Li, C. Polymerization on Heating up of Bio-Oil: A Model Compound Study. *AIChE Journal Reaction Engineering, Kinetics and Analysis* **2013**, *59*, 888−900.
(27) Diebold, J.; Czernik, S. Additives to Lower and Stabilize the Viscosity of Pyrolysis Oils During Storage. *Energy Fuels* **1997**, *11*, 1081−1091.
(28) Meng, J.; Smirnova, T.; Song, X.; Moore, A.; Ren, X.; Kelley, S.; Park, S.; Tillotta, D. Identification of Free Radicals in Pyrolysis Oil and Their Impact on Bio-oil Stability. *RSC Adv.* **2014**, *4*, 29840−29846.
(29) ASTM International. *Standard Test Method for Cleanliness and Compatibility of Residual Fuels by Spot Test*; 2019.
(30) Abdullah, H.; Mourant, D.; Li, C.; Wu, H. Bioslurry as a Fuel. 3. Fuel and Rheological Properties of Bioslurry Prepared from the Bio-oil and Biochar of Mallee Biomass Fast Pyrolysis. *Energy Fuels* **2010**, *24*, 5669−5676.
(31) Wang, Y.; Wang, Z.; Li, S.; Lin, W.; Song, W. Experimental Study of Rheological Behavior and Stream Gasification of Coal Bio-oil Slurry. *Energy Fuels* **2010**, *24*, 5210−5214.
(32) Badger, M.; Schobert, H. Viscosity Reduction in Extra Heavy Crude Oils. *Carbon* **1998**, *1*, No. 6.
(33) Keiser, J.; Bestor, M.; Lewis, S.; Storey, J. In *Corrosivity of Pyroloysis Oils*, Proceedings of the TAPPI PEERS Conference; 2011.
(34) Cubberly, W. *Metals Handbook, 9th Edition, Volume 1: Properties and Selection: Irons, Steels, and High-Performance Alloys*, 9th ed.; ASM International: Cleveland, 1975; Vol. *1*.

https://dx.doi.org/10.1021/acs.energyfuels.0c00721
Energy Fuels 2020, 34, 8403−8413